

Theoretical Investigation of the Proton Assisted Pathway to Formation of Cytochrome P450 Compound I

Danni L. Harris* and Gilda H. Loew

Contribution from the Molecular Research Institute, 845 Page Mill Road, Palo Alto, California 94304

Received March 30, 1998. Revised Manuscript Received July 6, 1998

Abstract: Functional and dysfunctional enzymatic pathways of cytochrome P450s after formation of the reduced ferrous dioxygen species have been investigated using nonlocal density functional quantum chemical methods, employing a methyl mercapto iron porphine model of the cytochrome P450 heme complex. The goal of this study was to assess the validity of proposed pathways to both compound I and peroxide involving protonation of the distal and proximal oxygen atoms of the reduced ferrous dioxygen species. Optimized geometries, energies, and electrostatic and electronic properties of each putative heme intermediate in these pathways were calculated and these properties examined for consistency with the proposed role of the intermediate in compound I or peroxide formation. Single protonation of the distal oxygen resulted in significant weakening of the O–O bond. Addition of a second proton to the distal oxygen and energy optimization led directly to compound I and water products, without any apparent activation barrier or formation of a diprotonated intermediate. These results provide direct robust support for the proton-assisted mechanism of dioxygen bond cleavage to form compound I. The dysfunctional pathway to the formation of peroxide was explored by examining the properties of the distal and proximal singly protonated species. The proximal tautomer is thermodynamically less favorable than the distal species by 18.4 kcal/mol. Electrostatic features of both singly protonated species suggest preferred proton delivery to the remaining unprotonated oxygen in each case, favoring peroxide formation. Moreover, addition of a second proton to either of these singly protonated species results in formation of a stable hydrogen peroxide heme complex. These results, taken together, suggest that the simultaneous availability of two protons on the distal oxygen is a requirement for P450 enzymatic efficacy, while *asynchronous* delivery of protons to the dioxygen site favors decoupling.

Introduction

Cytochrome P450s are a ubiquitous family of metabolizing heme proteins found in nearly all living species, including fungi, plants, bacteria, insects, and mammals. There are now more than 350 known isozymes. In mammals, mitochondrial P450s are involved in every step of steroid biosynthesis. Microsomal P450 isozymes, found mainly in the liver, are primarily responsible for xenobiotic metabolism but can either aid in their elimination or lead to toxic metabolites as a result of the P450 enzymatic chemistry. P450s catalyze a variety of reactions, such as aliphatic and aromatic hydroxylations, epoxidations, heteroatom oxidation, and N- and O-dealkylation, by transfer of a single active oxygen from the heme unit to substrates. The heme unit that is the site of the enzymatic activity of all P450s consists of an iron protoporphyrin IX complex with a completely conserved cysteine as the proximal axial ligand of the heme iron. The catalytically active species that transfers the oxygen atom to substrates is thought to be an oxyferryl ($\text{Fe}=\text{O}$) adduct of the heme unit called compound I, two oxidation states above the inactive ferric resting-state form.

Formation of the active P450 oxyferryl species from the inactive ferric resting form is believed to take place via a common mechanism for all P450 enzymes shown in Figure 1.¹ In this generally accepted mechanism, substrate binds to the ferric resting form, usually displacing most or all of the water

present in the binding site. The next step is an initial one-electron reduction, resulting in a substrate-bound ferrous heme species. Molecular oxygen, a requirement for activation, then binds as a ligand to the heme iron, forming a ferrous dioxygen species, the last of four intermediates stable enough to be characterized by a wide variety of spectroscopic measurements. A second one-electron reduction of the ferrous dioxygen form follows, resulting in formation of the twice-reduced ferrous dioxygen species, a transient species two oxidation states below the ferric resting form. This species rapidly forms water and compound I. This catalytically active species, in turn, then rapidly oxidizes substrates by transfer of the active oxygen atom to it, forming products and returning to the ferric resting form of the enzyme.

The steps in the common enzymatic cycle leading to the formation of compound I from the twice-reduced dioxygen species are the least understood aspects of P450 metabolism because they occur so rapidly and involve extremely transient intermediates. Thus, the pathway that has been proposed, shown as pathway A in Figure 2, has only been inferred from indirect experimental evidence. This evidence includes kinetic isotope effect measurements that have definitively demonstrated the requirement of two protons to form compound I from the reduced oxyferrous species.² In addition, earlier studies using isotopically enriched molecular oxygen established that the oxygen that is transferred to substrates is the “proximal” one, directly bound to the heme iron and that the other “distal” oxygen is involved in the concurrent formation of water.³

(2) Aikens, J.; Sligar, S. *J. Am. Chem. Soc.* 1994, 116, 1143–114.

(1) Ortiz de Montellano, P. R. *Oxygen Activation and Reactivity in Cytochrome P450: Structure, Mechanism, and Biochemistry*, 2nd ed.; Ortiz de Montellano, P. R., Ed.; Plenum Press: New York, 19 Chapter 8. pp 245–308.

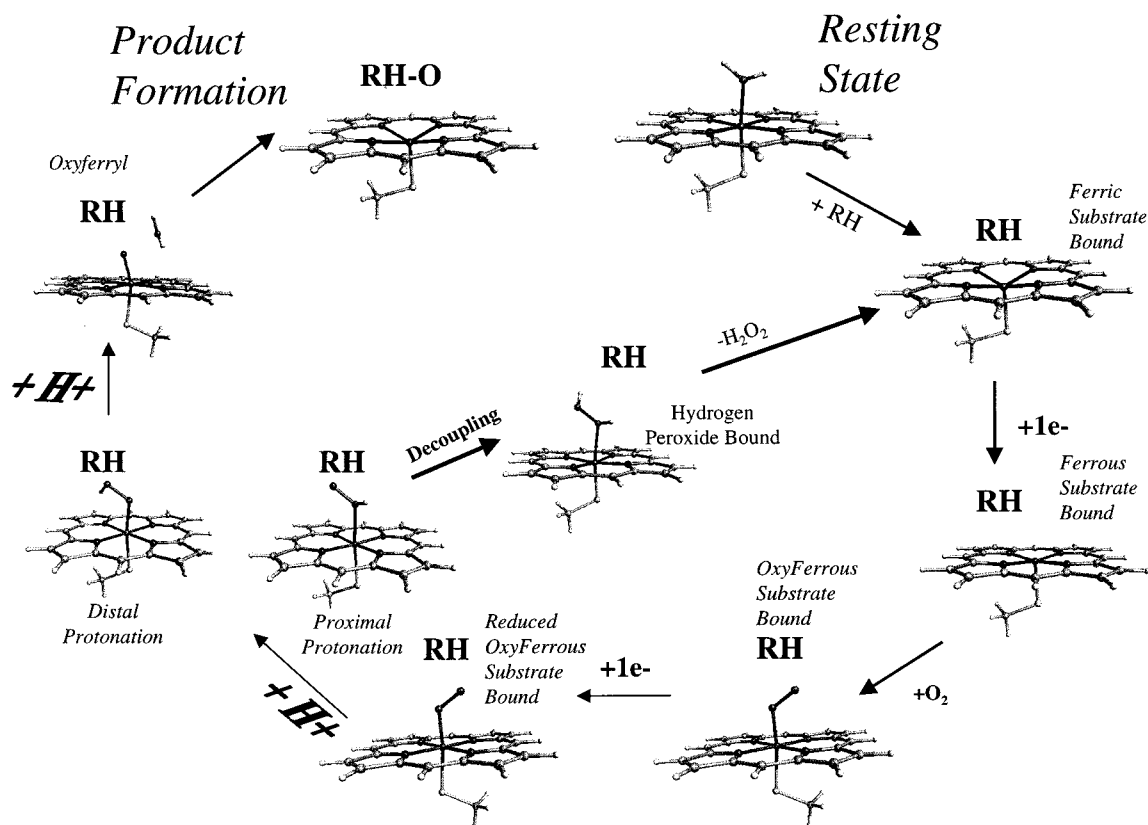


Figure 1. Enzymatic cycle of cytochrome P450s.

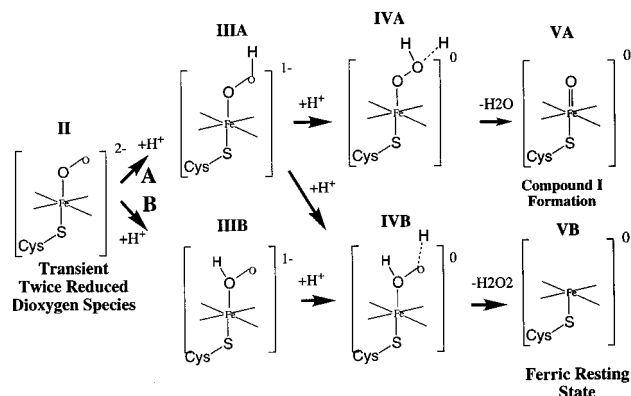


Figure 2. Hypothetical pathway to formation of compound I or hydrogen peroxide from the reduced ferrous dioxygen P450 species.

Based on these observations, as shown in Figure 2, pathway A, a proton-assisted mechanism of dioxygen bond cleavage has been proposed as the most likely pathway from the twice-reduced ferrous dioxygen species to compound I and water. This figure shows plausible individual steps in this proposed mechanism, involving sequential addition of two protons to the distal oxygen of the reduced ferrous dioxygen heme species, that can lead directly to the active oxyferryl (compound I) species and water. Although this mechanism is consistent with experimental observation and the typical mode of oxidation by transfer of a single oxygen atom to substrates, it is difficult from experiment alone to directly assess the validity of this pathway. A major impediment to further elucidation is that none of the transient intermediates invoked in this pathway following the ferrous dioxygen species have been characterized, including the reduced

ferric dioxygen species in its unprotonated, singly protonated, or doubly protonated forms, as well as compound I.

Variations in the distal binding site as well as substrate architecture can have dramatic effects on the branching between the normal pathway A, which leads to formation of compound I and water, and a decoupling pathway, B, also shown in Figure 2, that leads to generation of hydrogen peroxide and return of the heme to the ferric resting state. Pathway B is dysfunctional because, although molecular oxygen and two reduction equivalents are consumed, no product formation by monooxygenation of substrate occurs. As shown schematically in Figure 2, the proposed dysfunctional pathway B to peroxide formation proceeds from the same transient intermediate (II), the reduced ferrous dioxygen species, as does the formation of compound I. However, in contrast to compound I formation, protonation of both the proximal and distal oxygen atoms is required in order to form a hydrogen peroxide complex that can dissociate to yield the observed products, hydrogen peroxide, and the ferric resting state of the enzyme. As in the postulated pathway to formation of compound I, the proposed intermediates in this competing dysfunctional pathway have not been characterized experimentally.

A key role of the protein environment in the proposed pathways is to provide a source of stabilization of these transient oxy intermediates as well as to assist in the transfer of protons to the distal or proximal oxygen. Studies of P450cam and P450eryF, including both WT^{4,5} and mutant crystal structures,^{6,7} substrate variations,^{7,8} and mutations of amino acids,^{9,10} have

(4) Poulos, T. L.; Finzel, B. C.; Howard, A. J. *J. Mol. Biol.* **1987**, *195*, 687–700.

(5) Cupp-Vickery, J. R.; Poulos, T. L. *Struct. Biol.* **1995**, *2*, 144–153.

(6) Raag, R.; Martinis, S. A.; Sligar, S. G.; Poulos, T. L. *Biochemistry* **1991**, *30*, 11420–11429.

(7) Cupp-Vickery, J. R.; Han, O.; Hutchinson, C. R.; Poulos, T. L. *Nat. Struct. Biol.* **1996**, *3*, 632–637.

(3) (a) Atkins, W. M.; Sligar, S. G. *Biochemistry* **1988**, *27*, 1610–1616.
(b) Jones, J. P.; Rettie, A. E.; Trager, W. F. *J. Med. Chem.* **1990**, *33*, 1242–1246.

demonstrated that the binding site amino acid architecture and composition, the mode of binding and the nature of the substrate, and bound water can be important modulators of the competing delivery of protons to the distal and proximal oxygens that could determine the extent of coupling versus decoupling.

To probe the explicit role of the protein in the competitive P450 pathways requires knowledge of the structure of each P450. Previous molecular dynamics simulations of the reduced ferrous dioxygen species of two P450 isozymes with known structures P450cam¹¹ and P450eryF¹² have been performed to determine the likely proximal proton donors to the oxygen ligands, to help identify the ultimate source of protons, and to investigate the presence of dynamically stable H-bonded networks connecting them. While these empirical, energy-based, molecular dynamics studies were useful probes of the possible role of the protein in the enzymatic cycle, quantum mechanical methods are required in order to address the question of whether the intrinsic properties of the proposed intermediates are consistent with their proposed role in compound I and peroxide formation. To this end, nonlocal density functional methods have been used here to obtain the optimized geometries, relative energies, electronic structure, and molecular electrostatic potentials of each of the putative heme species in the reaction schemes indicated in both pathways A and B in Figure 2.

Nonlocal density functional theoretical methods are increasingly used as promising alternatives to computationally intensive correlated electron methods for a range of systems of biochemical interest. This method has been used to determine the optimized geometries for five-coordinate models of the oxyferryl heme complex¹³ and of iron-sulfur cluster models for active sites in proteins.¹⁴ It was also recently used to calculate the properties of compound I in peroxidases at experimentally determined geometries¹⁵ as well as to calculate the equilibrium geometries and electronic structure of a number of five- and six-coordinate iron porphyrin complexes with CO, O₂, imidazole, and NO as the proximal or distal ligands.¹⁶

A recent nonlocal DFT study has just been completed in our laboratory that further validates the use of this method for the specific model systems of interest here. In that study, nonlocal DFT was used to determine the ground-state geometries, spin multiplicities, and electrostatic properties of the ferrous dioxygen and reduced ferrous dioxygen model P450 heme species.¹⁷ The calculated structure and ground-state spin multiplicity obtained for the ferrous dioxygen cytochrome P450 intermediate were in excellent agreement with experimental observation. The geometry of the reduced ferrous dioxygen species was determined to be analogous to the ferrous dioxygen form. The finding of a doublet ground state for the reduced ferrous

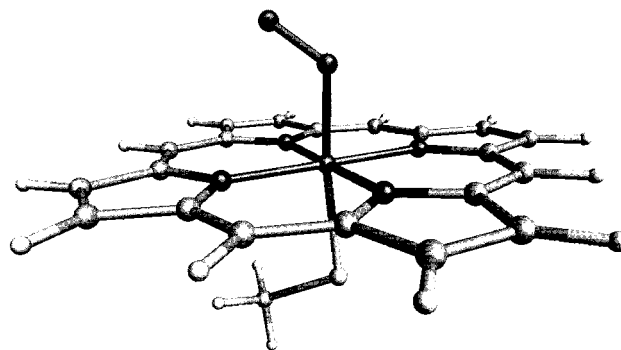


Figure 3. Optimized structure of the reduced ferrous dioxygen model P450 heme species.

dioxygen species is consistent with a reported ESR of this transient species. Finally, electronic spectra calculated using the *semiempirical* INDO/S/CI procedure, at the DFT optimized geometries of the ferrous dioxygen and the reduced ferrous dioxygen intermediate, resulted in spectral shifts completely analogous to the experimental spectra attributed to these putative species.¹⁸

In the present study, the same nonlocal DFT method was used to characterize putative species in the proposed competitive pathways to compound I and peroxide formation involving single and double protonation of the distal and proximal oxygens of the reduced ferrous dioxygen species. The calculated properties have been examined for consistency with the proposed role of the intermediates in compound I or peroxide formation. The results provide an assessment of the intrinsic validity of these pathways for all P450s. They can also be used to parametrize full protein simulations of P450 enzymatic intermediate states in order to continue to address the role of the binding site environment of specific P450 isozymes in their formation and stabilization.

Methods

Model Used and Choice of Initial Geometries. The model of the P450 heme site used in all calculations is an unsubstituted iron porphyrin complex with a methyl mercaptide (SCH₃⁻) axial ligand for the heme iron. As shown in Figure 2, it is the second axial ligand of this complex that changes during the portion of the P450 enzymatic cycle under consideration. The first species (II) in this cycle, shown in Figure 3, is the energy-optimized reduced ferrous dioxygen mercapto porphyrin system obtained from previous DFT calculations.¹⁷ In those previous studies, a possible alternative structure, with a bridged dioxygen bound to the heme iron, was found to be of much higher energy (28 kcal/mol). Initial structures of the next two species, the reduced ferrous dioxygen species singly protonated at the distal (IIIA) and proximal oxygen (IIIB), were generated by addition of a proton to each of the oxygen atoms of this geometry-optimized reduced ferrous dioxygen species. These two initial species, protonated at the distal and proximal oxygen atoms, were then energy optimized. The optimized structures of each of these singly protonated species were then used to construct initial models of the two doubly protonated species (IVA and IVB), and these diprotonated systems were subjected to energy optimization.

Density Functional (DFT) Calculations. Density functional calculations were performed using DGauss version 4.0 in conjunction with the UNICHEM interface.¹⁹ All DFT calculations were performed using Becke's 1988 functional, which includes the Slater exchange along with corrections involving the gradient in the density (nonlocal corrections). The Perdew-Wang 1991 (BPW91)²⁰ gradient-corrected correlation functionals were used in this study, given their superior performance

(8) Kадkhodayan, S.; Coulter, E. D.; Maryniak, D. M.; Bryson, T. A.; Dawson, J. H. *J. Biol. Chem.* **1995**, *270*, 28042.

(9) Martinis, S. A.; Atkins, W. M.; Slayton, P. S.; Sligar, S. G. *J. Am. Chem. Soc.* **1989**, *111*, 9252.

(10) Imai, T.; Shimada, H.; Watanabe, Y.; Matsushima-Hibiya, Y.; Makino, R.; Koga, H.; Horiuchi, T.; Ishimura, Y. *Proc. Natl. Acad. Sci. U.S.A.* **1989**, *86*, 7823.

(11) Harris, D.; Loew, G. H. *J. Am. Chem. Soc.* **1994**, *116*, 11671-11674.

(12) Harris, D. L.; Loew, G. H. *J. Am. Chem. Soc.* **1996**, *118*, 6277-6387.

(13) Ghosh, A.; Almlof, J.; Que, L., Jr. *J. Am. Chem. Soc.* **1993**, *98*, 5576.

(14) Mouesca, J.-M.; Chen, J. L.; Noodleman, L.; Bashford, D.; Case, D. A. *J. Am. Chem. Soc.* **1994**, *116*, 11898.

(15) Kuramochi, H.; Noodleman, L.; Case, D. A. *J. Am. Chem. Soc.* **1997**, *119*, 11442-11451.

(16) Rovira, C.; Kunc, K.; Hutter, J.; Ballone, P.; Parrinello, M. *J. Phys. Chem.* **1997**, *101*, 8914-8925.

(17) Harris, D.; Loew, G.; Waskell, L. *J. Am. Chem. Soc.* **1998**, *120*, 4308-4318.

(18) Benson, D. E.; Suslick, K. S.; Sligar, S. G. *Biochemistry* **1997**, *36*, 5104-5107.

(19) DGauss 4.0/Unichem Oxford Molecular, Beaverton, OR.

(20) Perdew, J. P.; Wang, Y. *Phys. Rev. B* **1992**, *45*, 13244.

over other nonhybrid functionals in our previous studies.¹⁷ A double- ζ valence polarization DGauss basis (DZVP) set,^{21,22} employing atomic centered Gaussian basis functions optimized for use with DFT, was used in all calculations.

This program employs an additional auxiliary approximation in the use of the fitting basis²³ to express the charge density in a series expansion in Gaussian basis functions. The energy expression, employing this fitting basis, may be computed in order N^3 , in contrast to the exact energy expression, which scales as N^4 . Use of this approximation makes feasible full geometry optimization of intermediates of cytochrome P450s of unknown structure. Results in our laboratory for small molecules containing iron using this approximation were found to reproduce previous results obtained by Bauchlicher using couple cluster methods as well as experimental properties.

In all calculations, a fine density grid was chosen (ca. 107 844 grid points). All the SCF iterations were converged to 2×10^{-6} in the density matrix and 2×10^{-8} in the energy. All optimizations converged within the chosen criterion of 0.0008 hartrees/Å. All calculations were made using 2-CPU's of a J90 provided by Oxford Molecular (Beaverton, OR).

Iron porphyrin complexes in both model compounds and intact heme proteins have closely spaced, low-lying electronic states of different spin multiplicity, differing in the spin pairing in open shell iron orbitals. While density functional theory was originally cast for the ground state,²⁴ it is equally valid to apply it to the lowest excited states with different spin multiplicities and symmetries.²⁵ In the previous DFT calculations, the ground state of the ferrous dioxygen P450 heme species was found to be a closed shell singlet, while the ground state of the reduced ferrous dioxygen P450 heme species was found to be a doublet. In the continuing studies here, geometry optimizations were performed for both doublet and quartet states of the singly protonated reduced ferrous dioxygen P450 heme species, as well as for the peroxide-bound and compound I species. Specifically, an initial SCF was converged for each of these possible spin states of these intermediates. The structures were then subsequently optimized until a stationary point was located on each spin-state surface using the unrestricted density functional code embodied in DGauss. The structure and electronic description of the ground state were determined as the lower energy of the two spin-state alternatives for each species.

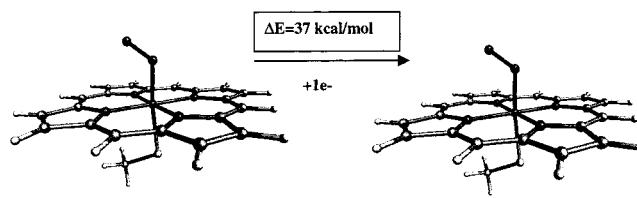
Proton affinities of the distal and proximal oxygen sites of the reduced ferrous dioxygen species were determined from the difference in energy between the optimized species with and without a proton. The DGauss code at present does not permit the calculation of basis set superposition error corrections to these calculated proton affinities. Estimates of the order of magnitude (1–1.5 kcal/mol) of these corrections from model iron oxygen systems, however, indicate the corrections to be small compared to the computed proton affinities of greater than 400 kcal/mol reported in this work. The values of the proton affinities, while computed at structures optimized to a stationary point, have also not been corrected for zero-point energy, given the size of the problem and computational limitations.

Mayer Bond Orders. The Mayer bond orders,²⁶ or charge density bond-order matrix elements, listed in tables for each of the intermediates in this work are defined in terms of the overlap matrices \mathbf{S} and the density matrices for the α and β spins, \mathbf{P}^α and \mathbf{P}^β , respectively. Mayer defined the bond order between atoms A and B as

$$B_{AB} = 2 \sum_{\nu \in A} \sum_{\nu' \in B} [(P^\alpha S)_{\nu\nu'} (P^\alpha S)_{\nu\nu'} + (P^\beta S)_{\nu\nu'} (P^\beta S)_{\nu\nu'}]$$

The Mayer bond orders are particularly useful criteria of bond strength since their values are close to those implied in traditional chemical structure representations. For example, the calculated value

Table 1. DFT Optimized Geometries^a and Bond Orders for Oxyferrous and Reduced Oxyferrous Porphine



| geometric quantity | oxy-ferrous | bond order (Mayer) | reduced ferrous dioxygen | bond order (Mayer) |
|----------------------|-------------|--------------------|--------------------------|--------------------|
| Fe–O1 | 1.82 | 0.95 | 1.95 | 0.38 |
| O1–O2 | 1.31 | 1.20 | 1.33 | 0.87 |
| Fe–N1 | 2.01 | 0.62 | 2.03 | 0.30 |
| Fe–N2 | 2.01 | 0.64 | 2.01 | 0.31 |
| Fe–N3 | 2.04 | 0.64 | 2.03 | 0.31 |
| Fe–N4 | 2.04 | 0.62 | 2.03 | 0.30 |
| Fe–S | 2.32 | 0.95 | 2.46 | 0.35 |
| C2–S | 1.84 | 0.99 | 1.85 | 0.51 |
| \angle Fe–O1–O2 | 122 | | 120 | |
| \angle S–Fe–O1 | 173 | | 175 | |
| \angle C–S–Fe | 110 | | 109 | |
| \angle N4–Fe–O1–O2 | 45 | | 45 | |
| \angle C–S–Fe–N4 | 45 | | 45 | |

^a Distances in angstroms and angles in degrees.

of the Mayer bond order for a localized double bond would be close to 2. In addition, the bond orders defined in this manner are superior to Mulliken bond orders in that they are less basis set dependent and may be used to compare the effect of changes in similar molecules.

Results and Discussion

Effect of Second Electron Reduction of Cytochrome P450s: Comparison of the Structures of the Ferrous Dioxygen and Reduced Ferrous Dioxygen Species. No X-ray crystal structures have, as yet, been reported for postulated putative species following the second electron reduction of the ferrous dioxygen species in the enzymatic cycle of P450s due to their extremely transient nature. Crystal structures have been reported for several of the bacterial enzymes in a number of ferric substrate-bound and resting ferric heme forms. The ferrous CO P450*cam* crystal structure²⁷ is the only ferrous species of an intact P450 thus far reported.

Our previous study of the structure of the ferrous and reduced ferrous dioxygen species using nonlocal DFT and using BLYP and BPW91 exchange–correlation functionals indicates them to both involve “end-on” dioxygen-binding geometries.¹⁷ Results for these species, using the BPW91 functional, are repeated in Table 1, since they are the starting point for the present study. As shown in Table 1, the second electron reduction results in a species +37 kcal/mol less stable than the ferrous dioxygen form. The reduced ferrous dioxygen intermediate is, nevertheless, a bound, nondissociative species. As shown in this table, the main effects of reduction of the ferrous dioxygen species were the elongation of the Fe–S and Fe–O bonds by 0.14 and 0.13 Å, with a very small increase in the O–O bond of only 0.02 Å. While calculated Mayer bond orders indicate some O–O bond weakening from a value of 1.20 to 0.87 upon reduction of the ferrous dioxygen species, reduction alone is not sufficient for the cleavage of the dioxygen O–O bond required to form compound I.

Intermediates in the Proposed Pathway to Compound I and Peroxide Formation. The optimized geometries and relative energies of the distal and proximal singly protonated

(21) Godbout, N.; Salahub, D. R.; Andzelm, J.; Wimmer, E. *Can. J. Chem.* **1992**, *70*, 560.

(22) Sosa, C.; Andzelm, J.; Elkin, B. C.; Wimmer, E.; Dobbs, K. D.; Dixon, D. A. *J. Phys. Chem.* **1992**, *96*, 6630.

(23) (a) Dunlap, B. I.; Connolly, J. W. D.; Sabin, J. R. *J. Chem. Phys.* **1979**, *71*, 3396; (b) **1979**, *71*, 4993.

(24) Hohenberg, P.; Kohn, L. *J. Phys. Rev. B* **1964**, *136*, 864.

(25) Gunnarsson, O.; Lundqvist, B. I. *J. Phys. Rev. B* **1976**, *13*, 4274.

(26) Mayer, I. *Int. J. Quantum Chem.* **1986**, *29*, 73–84.

(27) Raag, R.; Poulos, P. *Biochemistry* **1989**, *28*, 7586–7592.

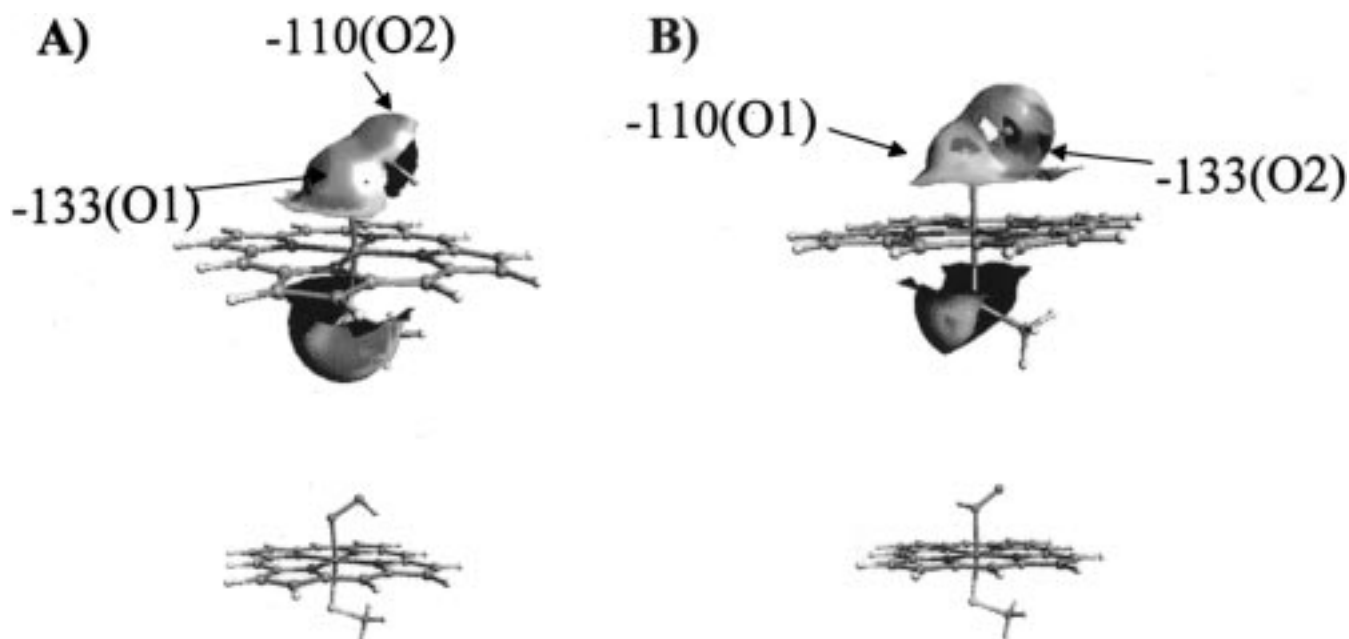


Figure 4. Molecular electrostatic potential surface (MEPS) of (A) distal protonated and (B) proximal protonated reduced ferrous dioxygen P450 heme species. The range of the molecular electrostatic potential plotted is indicated next to each representation. In each panel, the MEPS has been mapped to color ranges from blue (minimum) to red (maximum).

reduced ferrous dioxygen species are given in Table 2. These species retain the doublet ground state of the unprotonated form,¹⁷ but with different spin distributions, as shown in Table 4. The Fe–S bond is strengthened by protonation, as evidenced by its reduction in length by 0.14 Å for distal protonation and 0.19 Å for proximal protonation. As shown in the labeled figures associated with Table 2, both oxygen atoms have a large proton affinity, and protonation of each is highly exothermic, as is expected for protonation of a charged species. However, as also shown in the figure associated with this table, the distal protonated tautomer is thermodynamically favored by 18.4 kcal/mol over the proximally protonated form. As noted in the Methods section, the proton affinities in Figure 4 (and the figures in Table 2) have not been corrected for basis set superposition error. Estimates of the magnitude of this correction for the [Fe–O₂]⁺ system from model compound studies in our laboratory²⁸ as well as systems investigated by Komornicki and Dixon²⁹ indicate the corrections to be on the order of 1 kcal/mol and cannot account for the large difference between the distal and proximal proton affinities calculated in this study.

Protonation of the distal oxygen weakens the O–O bond and strengthens the Fe–O bond compared to the unprotonated reduced ferrous dioxygen species, as reflected in both bond length and Mayer bond orders shown in Table 2 and summarized in Figure 5. The weakening of the O–O bond is manifested by both a significant increase in the O–O bond by 0.13 Å and a decrease in the bond order from 0.87 to 0.48. The strengthening of the Fe–O bond is manifested in a decrease in the Fe–O bond length by 0.06 Å and an increase in bond order from 0.38 to 0.55. This significant O–O bond weakening upon even single protonation provides direct support for the proposed mechanism of proton-assisted dioxygen bond cleavage to formation of compound I. Further convincing support for this mechanism is provided by the finding that addition of a second proton to the distal oxygen does not result in a stable species. No minimum was found corresponding to this twice-protonated

Table 2. DFT Optimized Geometries^a and Bond Orders and Relative Energies^b of the Protonated Reduced Ferrous Dioxygen Porphine Species

| geometric quantity | distal protonated | bond order (Mayer) | proximal protonated | bond order (Mayer) |
|--------------------|-------------------|--------------------|---------------------|--------------------|
| Fe–O1 | 1.89 | 0.55 | 2.06 | 0.24 |
| O1–O2 | 1.46 | 0.48 | 1.41 | 0.56 |
| Fe–N1 | 2.03 | 0.28 | 2.00 | 0.31 |
| Fe–N2 | 2.03 | 0.31 | 2.03 | 0.31 |
| Fe–N3 | 2.02 | 0.33 | 2.03 | 0.32 |
| Fe–N4 | 2.02 | 0.30 | 2.01 | 0.31 |
| Fe–S | 2.32 | 0.58 | 2.27 | 0.58 |
| C2–S | 1.83 | 0.50 | 1.83 | 0.50 |
| ∠Fe–O1–O2 | 118 | | 127 | |
| ∠S–Fe–O1 | 170 | | 172 | |
| ∠C–S–Fe | 110 | | 109 | |
| ∠N4–Fe–O1–O2 | 57 | | –40 | |
| ∠C–S–Fe–N4 | 46 | | 50 | |

^a Distances in angstroms and angles in degrees. ^b All energies are in kcal/mol. ^c $\Delta E_{\text{prot}} = [E(\text{unprotonated}) - E(\text{protonated})]$.

species. Rather, the addition of the second proton leads directly and without any apparent energy barrier to the formation of compound I and water. As shown in Figure 5, this is also a very exothermic reaction ($\Delta E = -334$ kcal/mol), with the products, compound I and water, much more stable than the reactants, the singly protonated distal species and the second proton. These results, taken together, provide strong support for either consecutive or simultaneous double protonation of the distal oxygen as the preferred pathway to formation of compound I from the reduced ferrous dioxygen species.

(28) D. Harris, unpublished calculations.

(29) Komornicki, A.; Dixon, D. A. *J. Chem. Phys.* **1992**, *97*, 1087–1094.

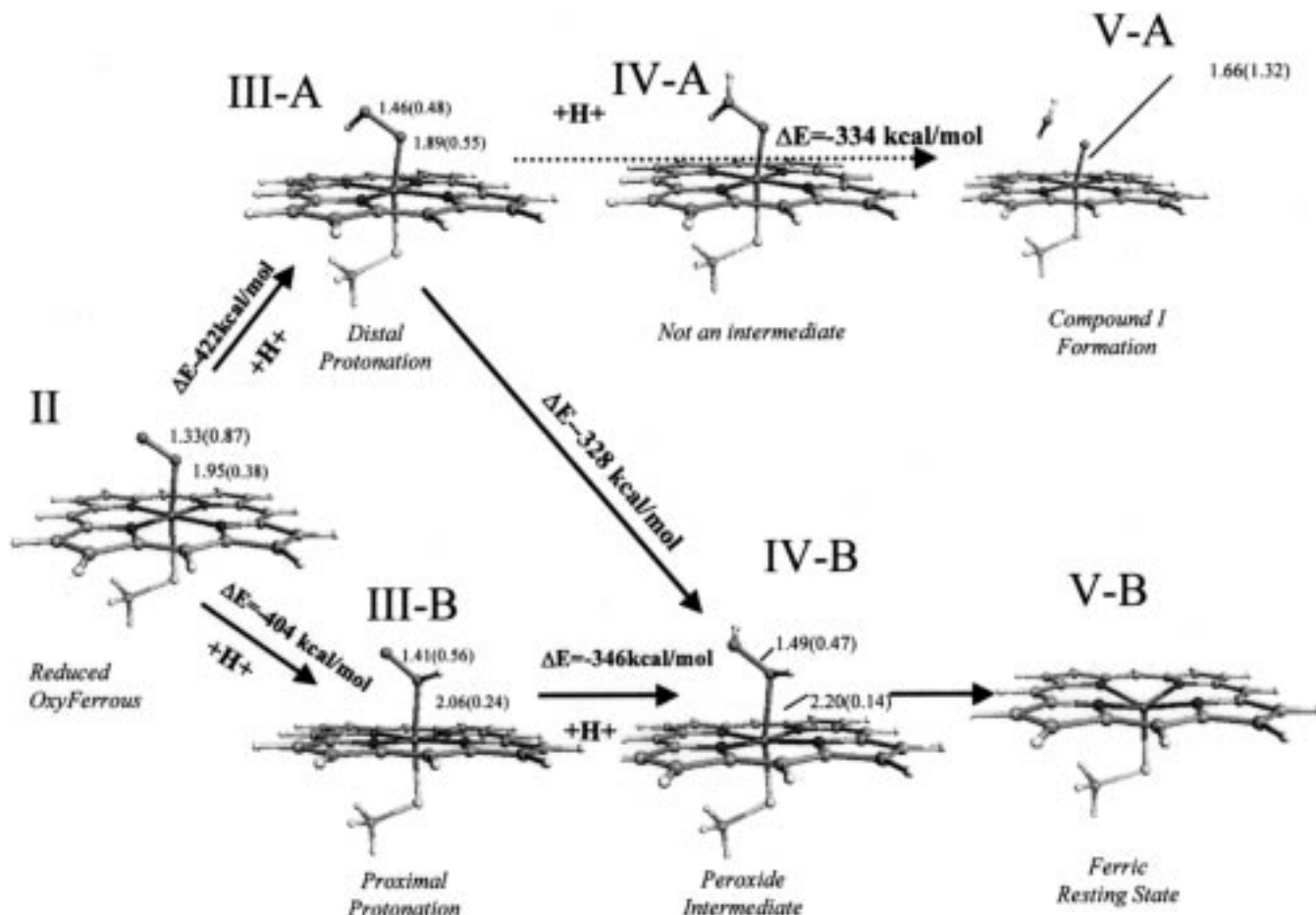


Figure 5. Summary of energy differences and principal bond length/order changes in the proposed competing pathways to compound I and peroxide formation.

In addition to further elucidation of the functional pathway to compound I formation, the results obtained also allow insight into the possible pathways for dysfunctional formation of peroxide observed for some substrates and mutants of specific cytochrome P450 isozymes after second electron reduction. As shown in Table 2 and Figure 5, protonation of the proximal oxygen weakens the Fe–O bond by lengthening it by 0.09 Å and reducing the bond order from 0.38 to 0.24. This result is consistent with the postulated role of this competitive protonation in the decoupled pathway. However, this tautomer is of significantly higher energy than the distally protonated species. Thus, it would play a significant role in the protein only if the substrates and mutants that cause decoupling lead to interactions in the protein binding site overcoming the thermodynamic disadvantage of formation of this proximal protonated species. For example, a particular arrangement of polar amino acids and bound waters in the binding site could favor hydrogen bonding to the proximal oxygen.

There is, however, an alternative pathway to peroxide formation that need not involve the less favorable initial protonation of the proximal oxygen. This pathway involves addition of a proton to the proximal oxygen of the more stable distal protonated species. The calculated molecular electrostatic potential surface (MEPS) around the protonated dioxygen ligand in these two species, shown in Figure 4, provides support for this hypothesis. As shown in this figure, in both singly protonated species, the electrostatic potential is about 20 kcal/mol lower near the oxygen that is unprotonated. This electrostatic potential difference should favor hydrogen bonding to the unprotonated oxygen site, with subsequent delivery of a proton

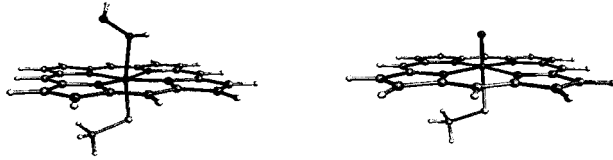
Table 3. Excess Spin Densities of Porphine Models of Putative Species in Pathway to Compound I and Peroxide Formation in Cytochrome P450s

| | spin population ^a on atoms | | | | |
|----------------------------|---------------------------------------|-------------------|---------------------|------------------|---------------------------|
| | reduced ferrous dioxygen | distal protonated | proximal protonated | peroxide complex | Compound I |
| Fe | -0.22 | 0.59 | 0.39 | 0.65 | 0.85 (1.03) |
| O1 ^b | 0.42 | 0.24 | 0.12 | | 0.92 (1.03) |
| O2 ^b | 0.51 | 0.06 | 0.36 | | |
| S | -0.02 | 0.18 | 0.19 | 0.37 | -0.56 (0.51) ^d |
| porphine A _{2u} π | 0.32 | | | | -0.21 (0.34) |

^a Mulliken open shell (unpaired spin) populations. ^b O1 is the proximal oxygen and O2 the distal oxygen. ^c Values in parentheses are for the quartet state. ^d Population on S in compound I in molecular orbital of mixed a_{2u}/S character.

to that site enhancing the fraction of reduction equivalents that culminates in the production of hydrogen peroxide.

Addition of a proton to the unprotonated oxygen in either singly protonated species leads to a stable peroxide-bound P450 model heme complex. Table 3 gives the optimized geometry of this peroxide complex in a doublet spin state. As can be seen in this table, the Fe–O bond in this species is considerably weakened from its value in either of the singly protonated forms, with the bond order reduced to the very small value of 0.13, making it a plausible precursor to peroxide formation. The H₂O₂ in the optimized peroxide-bound structure is nearly neutral, with a Mulliken charge of +0.11. There is a compensating negative charge on the porphine macrocycle. This charge distribution

Table 4. DFT Optimized Geometries^a and Bond Orders of the Hydrogen Peroxide-Bound and Compound I "Model P450 Heme Species"


| geometric quantity | hydrogen peroxide bound ($S = 1/2$) | bond order (Mayer) | oxoferryl ($S = 1/2$) ^b | bond order (Mayer) |
|---------------------|---------------------------------------|--------------------|--------------------------------------|--------------------|
| Fe–O1 | 2.20 | 0.13 | 1.66 | 1.31 |
| Fe–N1 | 2.00 | 0.33 | 2.00 | 0.33 |
| Fe–N2 | 2.02 | 0.33 | 2.00 | 0.33 |
| Fe–N3 | 2.04 | 0.33 | 2.05 | 0.33 |
| Fe–N4 | 2.01 | 0.33 | 2.05 | 0.33 |
| Fe–S | 2.16 | 0.88 | 2.37 | 0.40 |
| C2–S | 1.83 | 0.49 | 1.82 | 0.48 |
| O1–O2 | 1.49 | 0.47 | | |
| \angle Fe–O–O | 122 | | | |
| \angle N2–Fe–O | 92 | | 95 | |
| \angle S–Fe–O1 | 170 | | 170 | |
| \angle C–S–Fe | 110 | | 111 | |
| \angle H1–O1–Fe | 97 | | | |
| \angle O2–O1–H1 | 101 | | | |
| \angle H2–O2–O1 | 98 | | | |
| \angle S–Fe–O1–O2 | –154 | | | |
| \angle C–S–Fe–O1 | 167 | | | |
| \angle C–S–Fe–N4 | 138 | | 142 | |

^a Distances in angstroms and angles in degrees.

is clearly favorable for dissociation of this weakly bound complex to form hydrogen peroxide and a resting-state P450 heme species. This peroxide intermediate is also very close in energy to the products of the functional pathway (compound I + water), being only 6 kcal/mol higher in energy. These results strongly suggest that the bifurcation between functional product formation or dysfunctional peroxide formation could occur after single protonation of the distal oxygen atom, a thermodynamically favored pathway, rather than by initial competitive protonation of the proximal oxygen.

Structure of the Oxoferryl (Compound I) Species. Table 3 gives the optimized structure of the oxoferryl (compound I) P450 species based on a porphine template. The calculated ground state of this porphine compound I is a doublet, $^2A_{2u}$, with the lowest lying quartet state, $^4A_{2u}$, only 3 kcal/mol above the doublet. The structures of the oxoferryl form in the doublet and the quartet states are nearly identical, with the only pronounced difference being the length of the Fe–S bond. This bond length is 2.37 Å for the doublet state and 2.49 Å for the quartet. The Fe–O distances were 1.66 Å for the doublet and 1.67 Å for the quartet, with only minor differences in the other geometric parameters.

As shown in Table 4, the doublet and quartet states of the compound I species are also similar in that both arise from a total of three unpaired spins. In both the quartet and doublet cases, there are approximately two unpaired spins, of the same sign, distributed on the Fe and oxygen atoms. In both states, the third unpaired spin density is in a porphine πa_{2u} orbital that has significant admixture of the sulfur p-orbitals. This mixing results in substantial unpaired spin density on the sulfur as well. The salient difference between the two states is the manner in which the unpaired spin density ($S = 1/2$) on the porphine couples to the two unpaired spins ($S = 1$) on the iron and oxygen. In the doublet ground state, these spins are coupled in an antiparallel and, in the quartet, in a parallel fashion.

Although compound I of P450s is a transient species,

experimental evidence for this doublet ground state is provided by results for a very similar, but more stable, compound I heme complex with a mercaptide (cysteine) ligand formed by chloroperoxidase. Both Mössbauer resonance and electron spin resonance spectra have been reported for compound I of chloroperoxidase.^{30,31} These spectra have been interpreted in terms of an antiferromagnetic exchange-coupled Fe(IV) $S = 1$ and a spin $S' = 1/2$ porphyrin radical.³⁰ These results are consistent with the doublet state found here using the unrestricted nonlocal DFT for a compound I heme species with a mercaptide ligand that is common to both enzymes and with a local Xa single-point calculation of a methyl mercaptate compound I.³²

INDO/S semiempirical calculations of a model compound I using the DFT porphine compound I geometry also result in a $^2A_{2u}$ ground state, in complete agreement with the DFT results reported in this work. While recent evidence from Raman spectroscopy indicates a $^2A_{1u}$ ground state for chloroperoxidase,³³ there is no contradiction with the finding of a $^2A_{2u}$ ground state for the porphine compound I form in the present work. The disparity is not between computed and experimental results but in the heme sites involved. The calculations reported here are for a simple unsubstituted porphine compound I. The inferences drawn in the Raman spectroscopy are for the intact protein and, therefore, apply to the full protoporphyrin IX macrocycle with all its substituents. In fact, the addition of protoporphyrin IX substituents to the DFT porphine core compound I geometry does result in a calculated $^2A_{1u}$ ground state in recent INDO/S studies.³⁴ Thus, when the same heme species are compared, the results are in complete agreement. These results also demonstrate the sensitivity of the relative energies of the A_{2u} and A_{1u} compound I species to the nature and position of ring substitutions in porphyrins.

Conclusions

Density functional theoretical methods have been used to probe the nature and role of the putative oxy intermediates in a proposed pathway from the ferrous dioxygen species to formation of the catalytically active species common to all cytochrome P450, as well as the dysfunctional pathway to production of peroxide. In these studies, the heme model used was an unsubstituted iron porphine complex with a methyl mercaptate bound to the iron porphine. Employing this correlated electron method, we have reported the energy-optimized structures of the plausible putative intermediate forms, as well as determined the ground-state spin multiplicities and electrostatic potential surfaces of these species. The relative energies and geometric changes due to (1) second electron reduction of the ferrous dioxygen species, (2) distal oxygen protonation, (3) proximal oxygen protonation, and (4) addition of a second proton to the distal and proximal oxygens have been determined.

The computed optimized structure of the reduced ferrous dioxygen species results in an end-on binding mode, rather than a bridged one, analogous to both experimental^{35,36} and DFT calculations of the ferrous dioxygen intermediate.¹⁷ Addition

(30) Rutter, R.; Hager, L. P.; Dhonau, H.; Hendrich, M.; Valentine, M.; Debrunner, P. *Biochemistry* **1984**, *23*, 6809–6816.

(31) Rutter, R.; Hager, L. P. *J. Biol. Chem.* **1982**, *257*, 7958–7961.

(32) Antony, J.; Grodzicki, M.; Trautwein, A. X. *J. Phys. Chem.* **1997**, *101*, 2692–2701.

(33) Hosten, C. M.; Sullivan, A. M.; Palaniappan, V.; Fitzgerald, M. M.; Terner, J. J. *J. Biol. Chem.* **1994**, *269*, 13966–13978.

(34) D. Harris, unpublished calculations, manuscript in preparation.

(35) Dawson, J. H.; Kau, L.-S.; Penner-Hahn, J. E.; Sono, M.; Eble, K. S.; Bruce, G. S.; Hager, L. P.; Hodgson, K. O. *J. Am. Chem. Soc.* **1986**, *108*, 8114.

of this second electron results in a species 37 kcal/mol higher in energy than the ferrous dioxygen form. However, this reduced species is a viable intermediate form, albeit highly reactive and, therefore, extremely transient. The main geometric effect of second electron reduction is elongation of the Fe–O and Fe–S bonds with no appreciable change in the O–O bond. Thus, second electron reduction alone is not sufficient to lead to facile dioxygen bond cleavage. DFT optimizations of the reduced ferrous dioxygen species indicate the ground state to be a doublet, with one unpaired electron distributed over both the distal and proximal oxygen atoms. The computed ground-state spin multiplicities of the oxyferrous and reduced oxyferrous species are consistent with the reported ESR data for these species.^{37,38}

The computation of the ground-state structures of the single protonated distal and proximal reduced ferrous dioxygen species indicates them to be plausible intermediate species on the P450 reaction pathway. The proximal and protonated reduced oxyferrous species are both doublet ground states with unpaired electron spin density distributed mainly over both bound dioxygen atoms, but with some excess spin density on the Fe and S atoms. The principal effect of distal protonation of the reduced ferrous dioxygen form is O–O bond weakening, in keeping with its postulated role in facilitating O–O bond cleavage. By contrast, the principal effect of proximal protonation of the reduced ferrous dioxygen species is Fe–O bond weakening. This effect is consistent with its possible role in peroxide formation. However, both singly protonated species are found to be electronic bound states and, as such, are not spontaneously dissociative. Thus, the DFT calculations in this study confirm that neither the reduction step alone nor single protonation results in a species which spontaneously converts to the oxyferryl (compound I) species. Rather, these calculations indicate that diprotonation of the distal oxygen leads to spontaneous formation of the oxyferryl species, confirming the proposed functional pathway to oxyferryl formation. This result is consistent with the experimental kinetic isotope measurements² that indicate the requirement of two protons in the conversion of the reduced ferrous dioxygen species to compound I. By contrast, diprotonation in the form of proton addition at both the proximal and distal oxygens appears to be the principal prerequisite for hydrogen peroxide production in the decoupling of the enzymatic pathway.

Given the possibility that the addition of protons to the reduced ferrous dioxygen species of cytochrome P450s may be sequential rather than synchronous, the molecular electrostatic potential surfaces of both the distal and proximal protonated reduced ferrous dioxygen were calculated. The results indicate that, for both species, hydrogen bond formation to the previously

unprotonated oxygen would be favored, a feature likely to enhance its protonation, leading in each case to formation of the hydrogen peroxide complex. Thus, the extent of asynchronicity in the protonation steps could facilitate the decoupling of the P450 enzymatic cycle. If double protonation of the distal oxygen atom occurs nearly synchronously, compound I formation is clearly favored. If single protonation of the distal oxygen or the proximal oxygen occurs first, then second protonation leads to enhanced hydrogen peroxide formation. Given the more favorable formation of the once-protonated distal oxygen species, in the absence of specific effects of the protein environment, it appears that formation of this species could be the crucial bifurcation point between compound I formation and decoupling.

The ground state of the unsubstituted oxyferryl (compound I) porphine model species calculated by DFT is determined to be a ${}^2A_{2u}$ state with a low-lying quartet (${}^4A_{2u}$) 3 kcal above it. Thus, in the present DFT study, all of the species in the pathway to compound I formation retain the doublet ground state of the reduced ferrous dioxygen P450 heme species, for which there is also experimental evidence based on transient ESR and optical spectra.^{18,37} Both the doublet and quartet species have electronic configurations characterized by three unpaired spins two ($S = 1$) distributed over the Fe and O centers and a single electron ($S = 1/2$) distributed in the porphine a_{2u} orbital, a significant portion of which includes mixing of sulfur. The two states differ, in this unrestricted spin treatment, with respect to the sign of the net spin on the a_{2u} orbital.

The DFT result of a ${}^2A_{2u}$ compound I ground state is consistent with INDO/S calculations for the same geometry. With addition of porphyrin substituents corresponding to protoporphyrin IX in the intact proteins to the porphyrin ring in the optimized geometry derived from the DFT, the INDO/S ground state is a ${}^2A_{1u}$ ground state.³⁴ Thus, the observation of marker bands indicating a doublet ${}^2A_{1u}$ radical cation compound I porphyrin species in chloroperoxidase³³ is consistent with these results for a model system containing the same heme species.

The results of this study illustrate that density functional theoretical methods can be useful in characterizing the pathway to formation of crucial, catalytically active species of enzymes mediating the metabolism of xenobiotics in living systems, even when these pathways involve putative transient intermediates that have not been directly observed experimentally.

Acknowledgment. The authors acknowledge the support of NIH-GM 56125 for this research and the generosity of Oxford Molecular both for providing access to DGauss/Unichem 4.0 and for computer time on the Oxford Molecular Cray-J90.

Supporting Information Available: Table of the density functional energies for each of the species considered in this work (1 page, print/PDF). See any current masthead page for ordering information and Web access instructions.

JA981059X

(36) Schappacher, M.; Ricard, L.; Fischer, J.; Weiss, R.; Bill, E.; Montiel-Montoya, R.; Winkler, H.; Trautwein, A. X. *Eur. J. Biochem.* **1987**, *168*, 419–430.

(37) Davydov, R.; Kappl, R.; Huttermann, J.; Peterson, J. A. *FEBS* **1991**, *295*, 113.

(38) Kobayashi, K.; Iwamoto, T.; Hond, K. *Biochem. Biophys. Res. Commun.* **1994**, *201*, 1348.